Peer-reviewed version available at *Water* **2019**, *11*, 2051; doi:10.3390/w11102051

Article

Validation of A Novel, Shear Reynolds Number Based Bed Load Transport Calculation Method for Mixed Sediments Against Field Measurements

Gergely T. Török [1,2,*], Sándor Baranya [2] and János Józsa [1,2]

[1] MTA-BME Water Management Research Group; Hungarian Academy of Science—Budapest University of Technology and Economics, Műegyetem rakpart 3, H-1111 Budapest

[2] Department of Hydraulic and Water Resources Engineering, Faculty of Civil Engineering, Budapest University of Technology and Economics, Műegyetem rakpart 3, H-1111 Budapest

* Correspondence: torok.gergely@epito.bme.hu; Tel.: +36-1-463-2248

Abstract: In this study, the field measurement-based validation of a novel sediment transport calculation method is presented. River sections with complex bed topography and inhomogeneous bed material composition highlight the need for an improved sediment transport calculation method. The complexity of the morphodynamic features can result in the simultaneous appearance of the gravel and finer sand dominated sediment transport (e.g. parallel bed armoring and siltation) at different regions within a shorter river reach. For the improvement purpose of sediment transport calculation in such complex river beds, a novel sediment transport method was elaborated. The base concept of it is the combined use of two already existing empirical sediment transport models. The method was already validated against laboratory measurements. The major goal of this study is the verification of the novel method with a real river case study. The combining of the two sediment transport models is based on the implementation of a recently presented classification method of the locally dominant sediment transport nature (gravel or sand transport dominates). The results are compared with measured bed change maps. The verification clearly refers to the meaningful improvement in the sediment transport calculation by the novel manner in case of spatially varying bed content.

Keywords: bed load transport; shear Reynolds number; bed-armoring; bed-change; Danube; gravel-sand mixture; 3D CFD modeling

---

1. Introduction

Sediment transport modelling is a recently still developing topic of morphodynamic investigations. Although researchers elaborate increasingly accurate description of the sediment motion, there is still no one generally accurately applicable sediment transport model. The selection of the applied appropriate sediment transport method for a given case with even unique morphodynamic features must be preceded by a careful preliminary examination. There are, however, a large amount of empirically derived bed load transport formulas. A comprehensive collection of the most widely applied formulas can be found in Sedimentation Engineering Handbook [1]. The collection contains the most relevant sediment transport models, such as the ones from Meyer-Peter and Müller [2] from Einstein [3], Ashida and Michiue [4], Parker, Klingeman and McLean [5], surface-based relation of Parker [6], two-fraction relation of Wilcock and Kenworthy [7], surface-based relation of Wilcock and Crowe [8], relation of Wu et al. [9] and of Powell et al. [10]. The summary provides a short description of the hydraulic and sediment conditions of the experiments for which the given bed load formulas were developed. These conditions thus actually define the applicability limits of the formulas.

Török et al. [11] elaborated a novel calculation method, which does not represent a new sediment transport model. The method says that by the combined and parallel application of the present models the applicability range can be increased. This is a meaningful improvement of the accuracy of the sediment transport calculation, which was evidenced with laboratory measurements based validation [11]. However, the novel method was not yet verified with field measurements based comparative investigation.

2. Case study

A problematic reach of the upper Hungarian Danube reach (rkm 1796 – rkm 1794, **Error! Reference source not found.**) has undergone major morphological changes during the last decades. Many studies presented [12–18] that because of installations of many river regulation measures (e.g. groin fields, ripraps and hydropower plant at rkm 1819) in the last decades, intensive gravel formations [18], important bed level incision [19] and bed armoring processes [15,18] could be detectable, mainly in the main channel [20]. In contrast, the bed content is much finer in the groin fields, causing siltation and erosion of the finer sediments during flood waves [18,21].

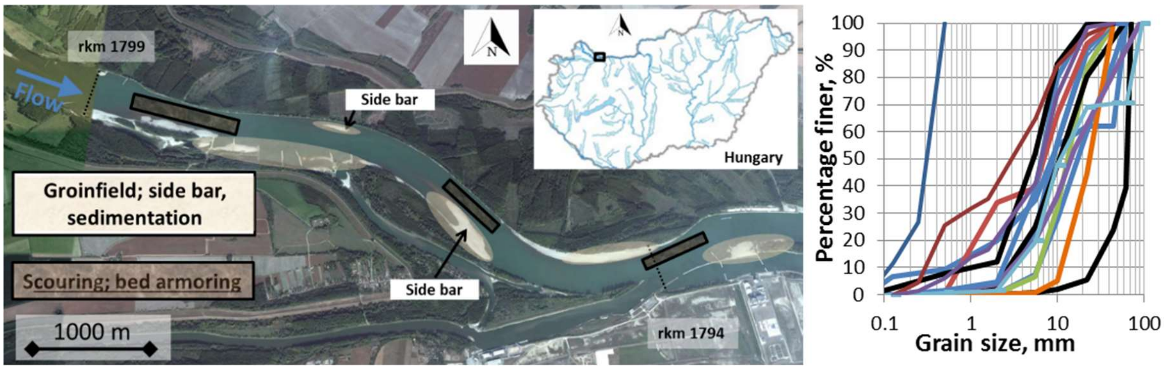

Figure 1. The sketch of the investigated Danube study reach (left) and grain size distributions taken from the investigated reach (right). The characteristic water discharges are Q_m = 2000 m³/s (mean flow), Q_{bf} = 4300 – 4500 m³/s (range of bankfull discharge) Q_2 = 5950 m³/s, Q_{10} = 7950 m³/s and Q_{100} = 10400 m³/s (2-, 10- and 100-year flood event) [19].

The river can be characterized by the following parameters: the channel bed width at mean water-stage ranges between 150 m and 350 m [18] with the average water surface gradient of 0.0002-0.00025. As **Error! Reference source not found.** shows, the river section is regulated by conventional structures, such as groins and the banks are protected against erosion by ripraps. Also, side arms, islands, gravel bars, confluence zone can be observed, which refer to the complex topography of the river section. Bed material samples were taken from the main stream, groin fields and gravel bars. Some of the grain size distributions can be seen in **Error! Reference source not found.**, right. The figures refer to very diverse spatial bed contents (0.32 mm < d_{50} < 70.5 mm. Such a wide dispersion of the bed content is a unique feature of the Danube River (~rkm 1600 - rkm 1800); at the lower Austrian Danube, (~rkm 1885, 90 km upstream), the Danube flows through a gravel bed, where d_{50} is 21.1 mm without any finer fractions [22]. In turn, the middle Hungarian Danube (~200 km downstream) has a typical sandy bed with d_{50} < 0.05 mm [23]. The complexity of the topography and bed content suggest spatially and temporally varied sediment transport nature [21]. That is in some places the gravel, elsewhere the sand transport dominates [24]. This kind of individual complexity was presented e.g. by the field measurements of Török and Baranya [18], or in [25,26].

The essential bed changes in the last decades caused important water management related problems and also difficulties in the navigation. For this reason, the reliable calculation of the morphological changes is a major interest to researchers and the application of a 3D CFD sediment transport model became justified. However, the choice of the applied sediment transport model was not obvious. Many formulas can be found in the literature (e.g. [2–4,27,28]). Most of them are developed focusing on a given morphodynamic process (e.g. Wilcock and Crowe model: bed armoring [8]; van Rijn model: sand erosion and deposition [29] etc…). However, in case of the examined river section, spatially and temporally varied sediment transport nature occur. That is,

Peer-reviewed version available at *Water* **2019**, *11*, 2051; doi:10.3390/w11102051

none of the existed sediment transport formula is expected to be operating reliably for both the sand and coarse bed material, within a given river reach.

3. Materials and methods

Introducing the combining sediment transport calculation method

Because of the complex and spatially varied bed material and dominant sediment transport nature, a novel combined approach [11] of the van Rijn and the Wilcock and Crowe bed load sediment transport formulas was applied. (From now, the Wilcock and Crowe formula will be indicated with *W&C*, while the van Rijn will be with *vR*.). The combined manner was already presented and validated against laboratory measurements [11]. Török and Baranya [21,24] pointed out a novel decision criteria, which is a suitable method for indicating whether the sand or rather the sand transport dominates locally. In this study, the combining of the two models bases on this statement. Namely, if the shear Reynolds number (Re^*) is below 300, the sand transport is prevalent. Otherwise, if the Re^* occurs above 400 the gravel transport dominates. Based on these, the combined calculation method says that the local bed load sediment transport rate is calculated as the followings ($q_{bi,W\&C}$ is the sediment transport rate calculated by *W&C* and $q_{bi,vR}$ is the rate by *vR*):

$$q_{bi} = \begin{cases} q_{bi,W\&C} \ if \ Re^* > 400 \\ q_{bi,vR} \ if \ Re^* \leq 300 \\ else \\ f \cdot q_{bi,W\&C} + (1-f) \cdot q_{bi,vR} \end{cases}, \tag{1}$$

where

$$= \frac{1}{100}(Re^* - 300). \tag{2}$$

Besides the bed load transport estimation, the suspended sediment transport is calculated in each computational grid according to the suspended *vR* formula [30]. Thus, the bed load is calculated according to Eq. 1 and 2, while the suspended load is estimated by the van Rijn equation.

Applied 3D flow model

The numerical model used in this study [31,32] solves the 3D Reynolds-averaged Navier-Stokes (RANS) equations with the *k-ε* turbulence closure (see e.g. [33]) by using a finite-volume method and the SIMPLE algorithm [34] on a 3D non-orthogonal grid. At the boundaries, where the fluid flow cannot be considered as a free turbulence zone, the wall law is applied for the velocity profile calculation [35]. The momentum equations are in the complete form, describing the hydrodynamic effects in all directions. The roughening impact of the vegetation in the flood plain area is described as an energy loss term in the Navier-Stokes equations [36], can be specified for each cell. Using this option, the effect of the vegetation was taken into account as a drag-effect.

Peer-reviewed version available at Water 2019, 11, 2051; doi:10.3390/w11102051

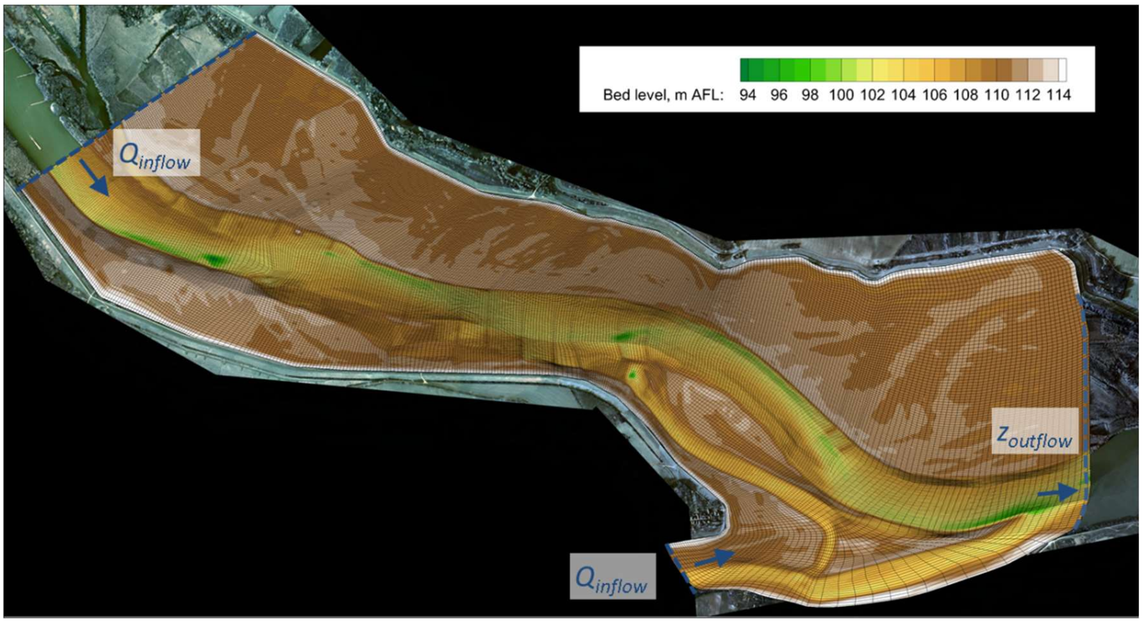

Figure 2. The computational grid of the investigated Danube study reach.

In order to eliminate the boundary effect, the computational grid was longer in both upstream (rkm 1801) and downstream (rkm 1793.5) direction than the investigated ~ rkm 1795 and rkm 1799 river reach. The applied grid can be seen in 0. The study side was discretized with 355 cells in the streamwise direction and 150 cells in the lateral direction, respectively, resulting in the streamwise direction in an average resolution of 18 m and transversely 5 m in the main channel, while 13 m in the floodplain area. Vertically 11 layers were defined.

The bed material was discretized by five fractions, which are: $d_1 = 0.3125$ mm, $d_2 = 1.25$ mm, $d_3 = 5.7$ mm, $d_4 = 16.2$ mm and $d_5 = 56.57$ mm. The ripraps and groins were characterized by $d = 300$mm. According to field measurement based considerations the active layer thickness was set to 0.5 m.

Parameterization

As e.g. [1] mentioned, the bed material of the most river reaches are less complex and the grain sizes happen in a narrow range. In turn, in rare cases - e.g. the herein studied river section – the occurring grain sizes cover a significantly wider range (silt - gravel), resulting in a very complex spatial distribution. Because of this, the bed material cannot be supposed as spatially uniform (as many study does at most river sections [37,38]), which makes the allocation of the bed material less obvious method. According to Baranya [39] a relation can be stated between the calculated local bed shear stress value by 3D flow model at the mean-water stage and the local d_{50}. Thus, based on the fitted function, a transitional and continuous d_{50} map can be estimated based on the calculated bed shear stress distributions. This methods was used, using 33 bed material samples [18,24]. The standard deviation of the calculated d_{50} to the measured d_{50} is 3.2 mm.

As the boundary conditions for the RANS equations, at the inflow boundaries the water discharge, at the outflow boundary the water level was set. The discharge time series (0) and the water levels of the Danube were defined based on the measured time series. Additionally, the flow discharge time series of the Mosoni-Danube was set based on a 1D numerical Danube model [40].

Preprints (www.preprints.org) | NOT PEER-REVIEWED | Posted: 1 August 2019

Peer-reviewed version available at Water 2019, 11, 2051; doi:10.3390/w11102051

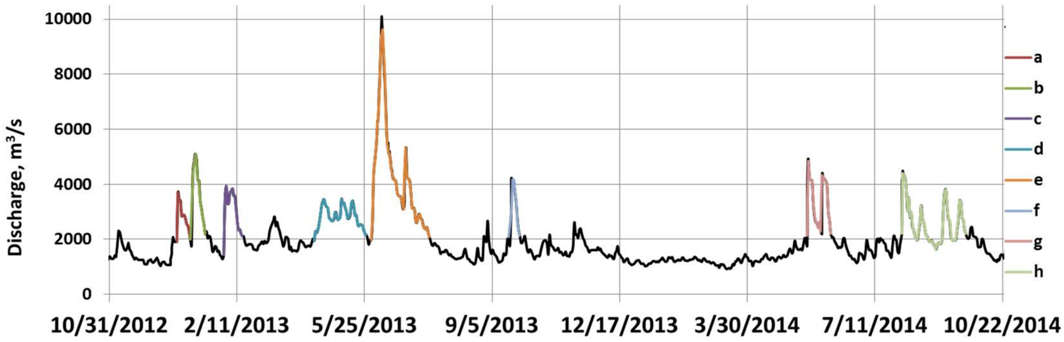

Figure 3. Discharge time series at rkm 1801 for the period 2012 October – 2014 October.

An essential part of the model setup is the correct set of the inflow sediment rate. For this purpose, the flow discharge dependence of the suspended load [41] and the bed load [18] functions were used.

The riverbed topography of the main river channel was available from 2012 and 2014. The initial bed geometry was set according to the map from 2012. The calculated bed change map could be prepared for this 2 years long period, which includes the historical flood wave from 2013 (0). This bed change map was used as benchmark for the validation purpose (0).

Four regions in the river reach were highlighted by green rectangles and an ellipse, marked by *A*, *B*, *C* and *D*. In these places, the following bed forms and morphodynamic processes were detected by field measurements [15,18]. At region *A* and *D*, the blue spots refers to a pronounced scouring downstream of the groins. At region B a groin field can be found. Here, local bed changes took place, both scouring processes (blue spots) and sediment depositions (brown spots). The ellipse (*C*) and the brown spot in region *D* shows the places where gravel bars are located. As these phenomena basically determine the reach-scale morphodynamic processes, a key question is whether the novel sediment transport calculation manner introduces a more reliably estimation of them.

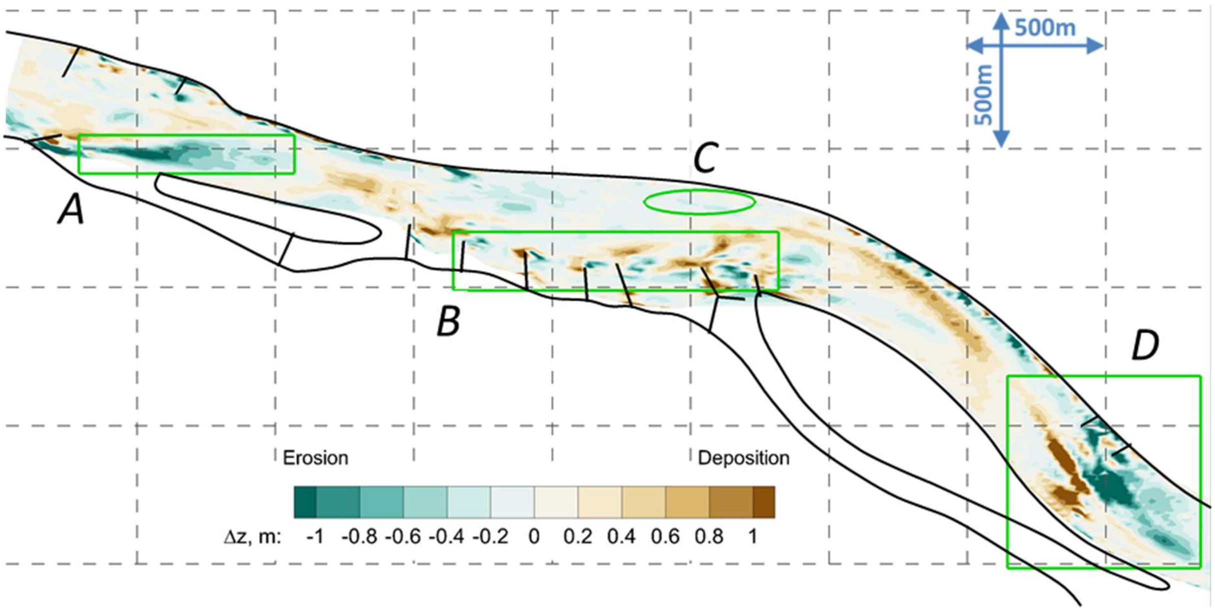

Figure 4. Measured bed changes for the period 2012 October – 2014 October.

The numerical simulation of the 2 years, 722 days long period demands very large computational capacity. According to the preliminary estimation calculations, the simulation of one model variant for such a long time period would take around half a year. Therefore, to reduce the duration of the simulation, only the periods which excess the bed-forming flow discharge (Q > 2100

Peer-reviewed version available at Water 2019, 11, 2051; doi:10.3390/w11102051

m³/s) [18,22] were simulated. In this range, 66% of the annual bed load amount passes [42]. Therefore, the major bed changes are expected during these periods. Accordingly, the bed changes caused by eight flood waves were calculated, which means a total of 211 days. In turn, it is emphasized that the ignored 34% of the annual bed load yield is significant. That is, the numerical model neglects the simulation of bed changes which take place during the lower water regime, so the results cannot be compared directly to the measured changes.

3D flow model validation

The herein applied 3D CFD model was already adapted and validated for the investigated Hungarian reach of River Danube, which were published in previous research works, e.g. [37,43–45]. Those studies have already demonstrated the reliable application of the 3D flow model. Regardless of these, the flow model validation was elaborated for the peak of the historical flood wave in 2013. The cross-sectional ADCP flow measurements by the North-Transdanubian Water Directorate regarding to the peak stage of the flood wave were used as benchmark flow values. 0 shows the measured (left) and the calculated (right) cross-sectional velocity distributions. Compared the measured and calculated cross-sections, a satisfactory match can be seen.

That is, the velocity values are in the same ranges (0-3 m/s). The highest velocities (yellow and red spots) are calculated at the same place of the cross-sections than in the real case, which underlines the reliable estimation of the main stream. The locations of the lower velocities (blue and light green spots) are calculated trustworthy also. That is the calculated flow pattern can be realised reliable at the groin fields (e.g. at the right-bank sides of cross-section III, IV and V, 0) and gravel bars also (e.g. at the right-bank sides of cross-section VII). Accordingly, the applied numerical flow model is considered to be validated for higher flood waves too, thus it is believed applicable for sediment transport modelling purpose.

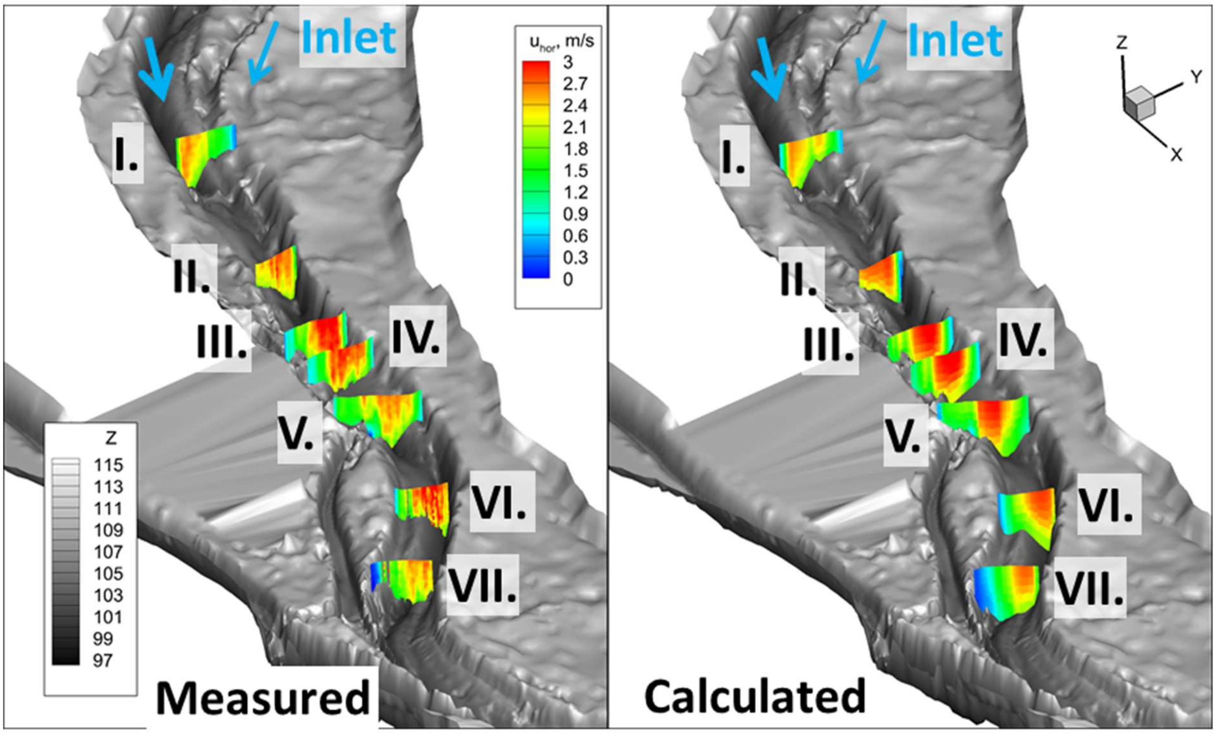

Figure 5. Measured and calculated cross-sectional horizontal velocity distributions.

Results

Comparison of the calculation methods

In order to confirm the better operation of the novel Re^* dependent combined method, the bed change calculation by the van Rijn, Wilcock and Crowe and the combined method were compared.

Because of the significant computational time, the simulations were performed only for the *d* and *e* flood waves (see. 0 *d* and *e*). The initial model setup (the flow field, water levels and the bed material) was given for each run from the results of the model run for the first three flood waves by the Re^* dependent combined method. The flood wave *d* is a relatively low (peak is around 3460 m^3/s), but durable (~2 months long) flood wave, while the *e* is the historical one with a peak higher than 10000 m^3/s. Thus, the comparative analysis presents the operational characteristics of the sediment transport models for both the durable lower and also for the extreme water regimes. As a benchmark the measured bed change map indicates the extent of the possible bed changes. However, the measured and calculated maps cannot be compared directly, because the measured belongs to the whole two year long period (0).

The bed change maps calculated for the flood wave d (0) by the *vR* model (0), by the *W&C* model (0) and also by the combined method (0) is presented. As the results show, the *vR* model estimates unrealistic changes both spatially and in magnitude. The unrealistically huge bed changes suggest that the *vR* model does not seem to be an appropriate model for the given Danube reach, particularly not for bed change calculation in the main channel.

The *W&C* sediment transport model estimates more stable bed surface than the *vR* (0). In this particular case the bed surface seems so resistant that the mean flow field is too weak to cause any significant bed changes. The motion of the very fine, basically suspended inlet load is calculated by the *W&C* model as bed load. Therefore, that part of the inlet sediments settled progressively along the channel. However, because of the quite low suspended load [41], the bed level rise caused by sedimentation is negligible (< 0.005 m).

0 shows the bed changes calculated by the combined method. The red lines illustrate the border line which separates the areas where the *vR* or the *W&C* model is activated in the initial moment of the model run. Accordingly it can be seen that the *vR* formula is invoked at the near-bank areas, at the groin fields and also at a smaller part of the Vének lower gravel bar. At these regions, more significant (~0.05 m) sedimentation is estimated. That is, at these less hydraulically rough parts of the river bed, the deposition of both the finer bed load and suspended load are expected, which areas can be detected by the Re^* [21]. In turn, in the navigation channel, no considerable bed change happened. According to the suspended form of the *vR* formula, the finer suspended load passes over the calculation domain, while the bed surface remains still, calculated by the *W&C* formula. This assumption is consistent with the conclusions of the field measurements [18]; the main channel seems to be armored enough to be resistant at mean water regime.

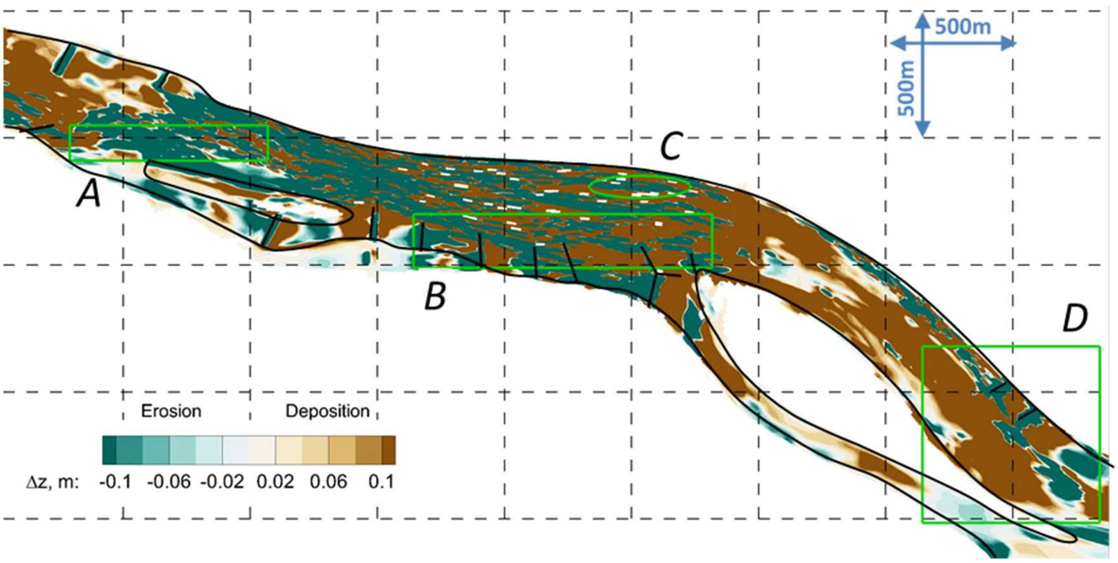

Figure 6. Calculated bed changes by the *vR* formula for a 2.5 month long period (0).

Peer-reviewed version available at *Water* **2019**, *11*, 2051; doi:10.3390/w11102051

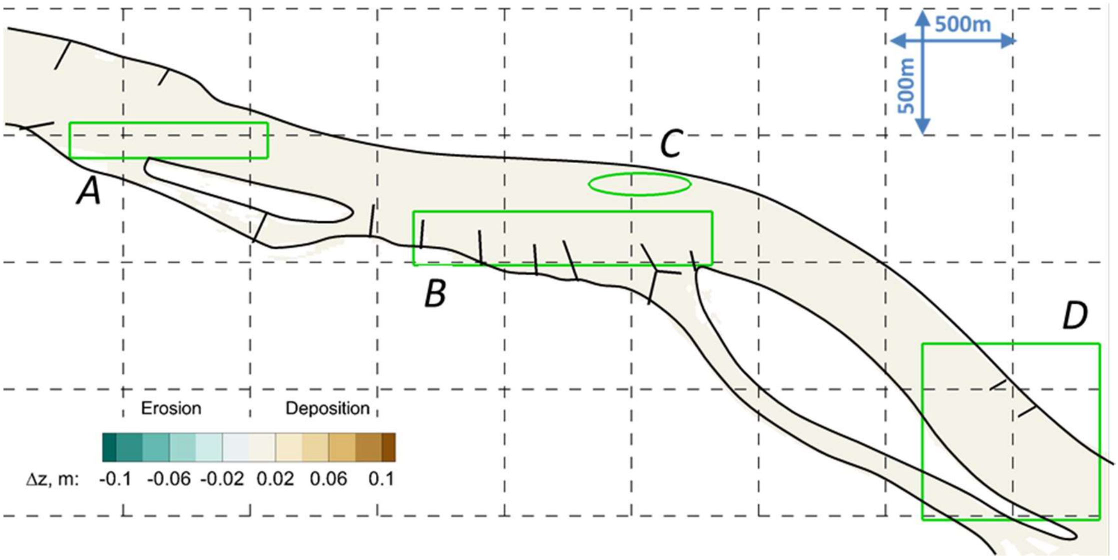

Figure 7. Calculated bed changes by the *W&C* formula for a 2.5 month long period (0).

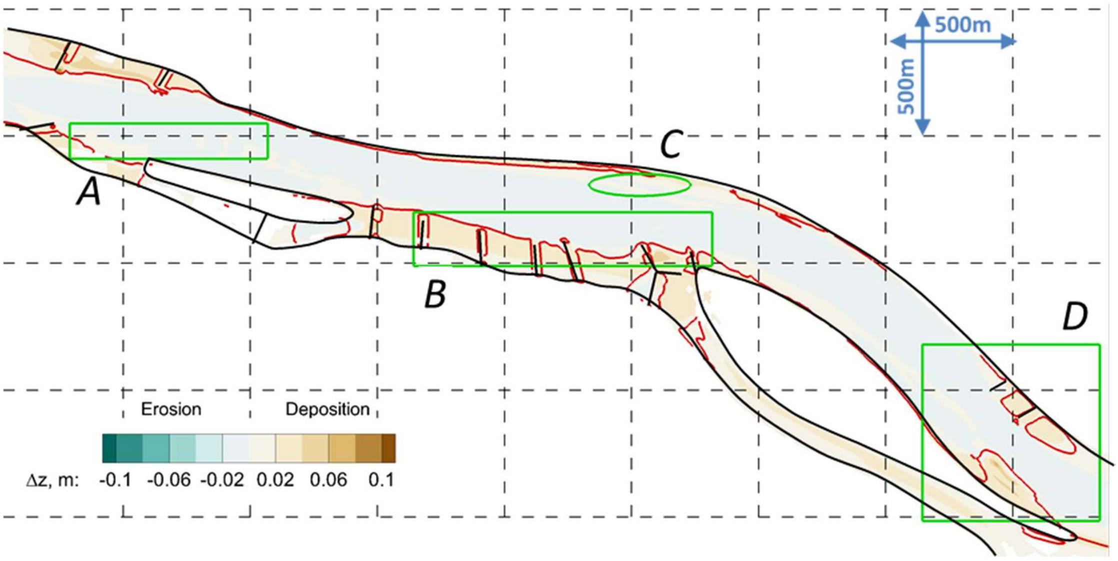

Figure 8. Calculated bed changes by the combined method for a 2.5 month long period (0).

The other flood wave, for which the comparative analysis were established is the historical flood wave from 2013 (0). Regarding to this hydrological case, the *vR* model estimates also an unrealistic bed change map (0). This is mainly true for the main channel. There, the motion of the coarser grains is probably overestimated, resulting in huge erosions and depositions. In turn, at the near-bank regions, at gravel bars and at the groin fields, the changes seem to be partly in the expectable order of magnitude. But it is clearly visible that the *vR* formula is not an appropriate choice for the morphological change calculation of such a complex river reach.

Peer-reviewed version available at *Water* **2019**, *11*, 2051; doi:10.3390/w11102051

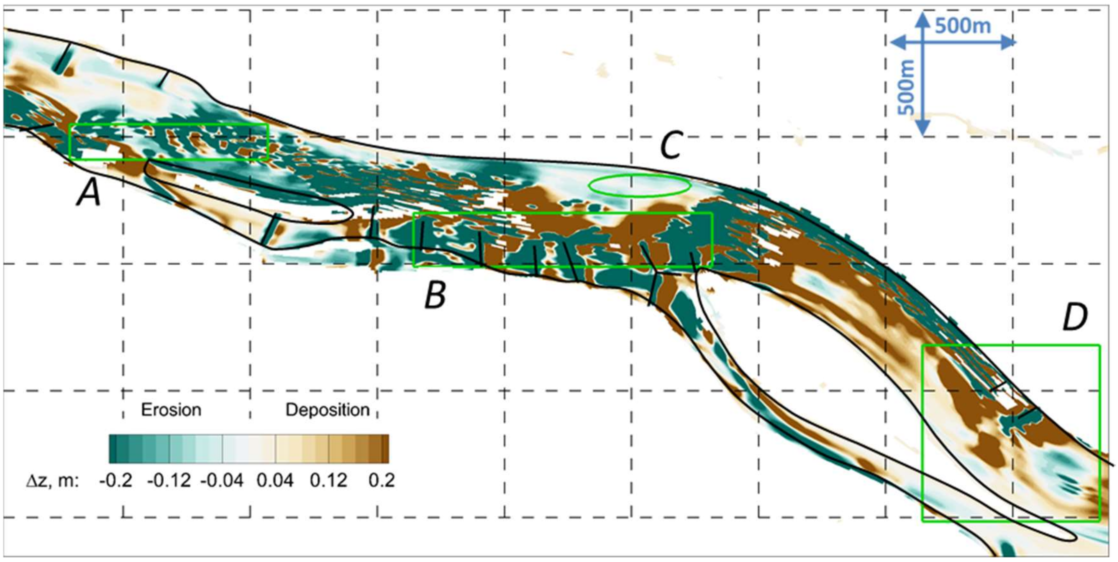

Figure 9. Calculated bed changes by the vR formula for the historical flood wave (0).

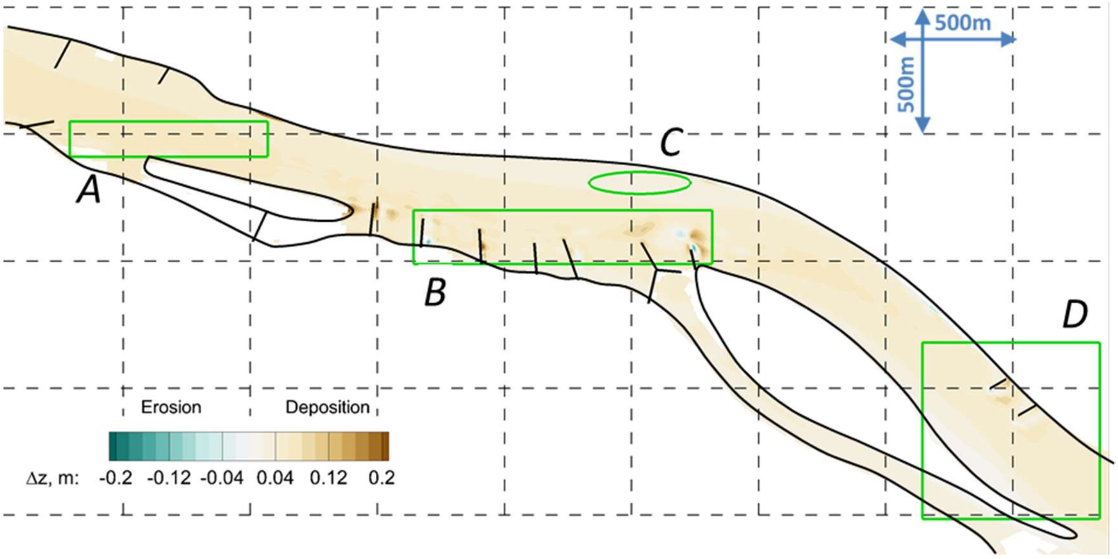

Figure 10. Calculated bed changes by the *W&C* formula for the historical flood wave (0).

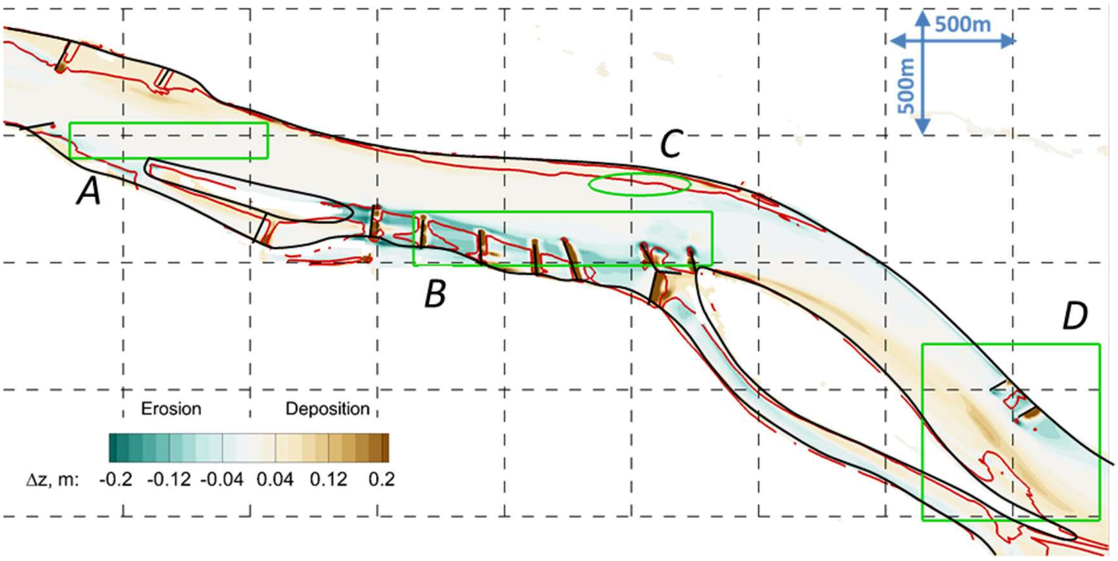

Figure 11. Calculated bed changes by the combined method for the historical flood wave (0).

The *W&C* model calculates more realistic bed changes (0), especially in the main channel. However, the measurements at the lower gravel bar and also at the whole main channel show significant ($\Delta z > \pm 0.2$ m) changes. Based on these, the *W&C* formula likely overestimates the stability of the channel. Remarkable bed level increase can be pointed out, which moderates towards the downstream direction. These bed level changes can be explained by the settling of the inlet finer load, which cannot be taken into account as suspended load. The publication of Török et al. [46] pointed out that in case of mixed bed content, the Shields diagram predicts lower critical bed shear stress for the bed load of the finer, sand particles, than the reference shear stress of the *W&C* model. Accordingly, the *W&C* model estimates respectively higher stability for the sand particles, than the Shields diagram and thus the *vR* model. This leads to the unrealistic deposition in the main stream.

The combined method predicts (0) more significant bed changes, compared to the one resulted by the *W&C* model. The red border line suggests that as at the flood wave *d*, the combined method calculates the sediment transport by the *vR* formula at the near-bank regions. During the flood wave *e*, the remarkable erosion at the groin field *B*. means that the groin field got flushed and the earlier deposited finer sands got eroded. Also notable changes took place at the vicinity of the gravel bar at region *D*. Here, the widening of the downstream sides of the gravel bar can be seen, in accordance with the measured bed change map in 0. Around the groin pair at the left bank, on the opposite side of the gravel bar, the blue spots refer to erosion. This process is probably the result of a similar, flushing process as the one which happened at the upstream groin field. In turn, in the main and navigation channel, no considerable bed change happened. According to the suspended form of the *vR* formula, the finer suspended load passes over the calculation domain, while the bed surface remains still, calculated by the *W&C* formula. The conclusions of the field measurements [18] referred also to resistant main channel.

The results indicate that the interactions between the sediment transport at different channel sections (groin fields, gravel bars and main channel) cannot be estimated by the *vR or W&C* formulas. But the expedient combination of them gives an opportunity to deal with the interaction-mechanism between the local- and reach-scale processes.

Analysing the calculated bed changes in the marked boxes, the following assumptions can be stated. In this part, the results of the *vR* model were skipped because of the unrealistic bed change calculations. At region *A*, the real bed level deepening (0) could not be reproduced by any method. At region *B*, only the combining method was able to predict significant depositions and erosions. Accordingly, the depositions probably take place during lower water regime, while the bed level incision occurs during the flood waves. Thus, the measured bed level changes during two years were formed most likely indeed during the whole two year long period. At region *C*, all two model results suggest that the gravel bar is in a stable state. Beside region *A*, the bed level increase in the main channel between region *C* and *D* (0) could not be pointed out by any sediment transport formula. Finally, at region *D* the model results show that the widening of the gravel bar and also the erosion at the vicinity of the groin pair occur rather during the higher flood wave than during the slighter flood waves, or mean water regime.

Measured data based verification of the combined method

A quantitative assessment of the tested sediment transport formulas was performed based on the results of the comparative analysis. First, in accordance with the conclusions of the field measurement based investigation it was assumed that the measured erosion and deposition took place mainly during higher water regimes at region *D*, when the flow discharge was higher than the bed forming discharge [18,42]. Thus, the measured and calculated data can be considered as indirectly comparable at this region. Therefore, from the measured bed level change maps, the total volume of the erosion and deposition can be calculated. Furthermore, counting the number of days of the higher water levels, the average daily rate of the volume of both the erosion and deposition

Peer-reviewed version available at Water 2019, 11, 2051; doi:10.3390/w11102051

can be estimated. Likewise, based on the calculated bed change maps and knowing the duration of the historical flood wave, the daily average volume changes of the deposition and erosion can be estimated. The following Table shows data about these volumes. The Table presents the ratio of the calculated and measured deposition and erosion volumes, for each sediment transport formula. A value of 1 would indicate a perfect match to the measured volume change.

Table 1. The $\Delta V_c/\Delta V_m$ values for region *D*, where ΔV is the average daily volume changes. ΔV_c is derived from the model results, while ΔV_m estimated from the bed level measurements.

		Sediment transport model		
		van Rijn	**Wilcock and Crowe**	**Re* based combined**
ΔV / day	**Deposition**	48.7	4.9	3.5
	Erosion	7.2	0	0.7

The Table data show, that the *vR* model is the one which overestimates most both the deposition and erosion volumes. The *W&C* model calculates the deposition rate more accurately, but still indicates more than the measured. This is partly explained by the lack of the suspended sediment calculation. In turn, the *W&C* model estimates negligible low erosion. In total, the more reliable results were provided by the combined method. With this, the erosions at the near-bank parts were calculated more accurately by the *vR* model, resulting in sediment feed for region *D*. Thus, because of the capturing of the coming sediments, the widening of the deposition could be better represented. As the Re^* dependent criterion activated the *vR* formula at the groin pair, the bed level incision at its vicinity was also estimated better.

Even though the measured and calculated bed changes cannot be compared directly, the nature, the magnitudes and the locations of the remarkable bed changes suggest the greater aptitude of the combined method.

As it was discussed in Chapter Model setup, the low- and mean flow discharges transport is the third part of the annual bed load, which also plays a not negligible role in the sediment feed and so in the bed changes. Because of the calculated bed changes were elaborated only for the higher flow discharges (> 2100 m³/s. 0), the results cannot be compared with the measured changes directly. Therefore, to achieve a notionally common scale, the bed change values were normalized. That is both the measured and calculated bed changes got divided by the highest bed level decrease or increase value of the main channel:

$$\Delta z_{norm} = \begin{Bmatrix} if\ \Delta z > 0 \rightarrow \frac{\Delta z}{\Delta z_{max}} \\ else \rightarrow \frac{\Delta z}{|\Delta z_{min}|} \end{Bmatrix}, \tag{3}$$

Thus, the occurring values develops between -1 and 1, where 1 indicates the maximum deposition height along the river reach, while -1 belongs to the biggest erosion ($\Delta z_{max,meas} = 1.5\ m$, $|\Delta z_{min,meas}| = 1.8\ m$; $\Delta z_{max,calc} = 0.5\ m$, $|\Delta z_{min,meas}| = 0.25\ m$). The measured bed changes both the erosions and depositions were consequently higher than the calculated. That is the numerical model underestimates the magnitudes of the bed changes. This can be partly explained by the ignore of the third part of the annual bed load in the numerical model estimation.

Peer-reviewed version available at *Water* **2019**, *11*, 2051; doi:10.3390/w11102051

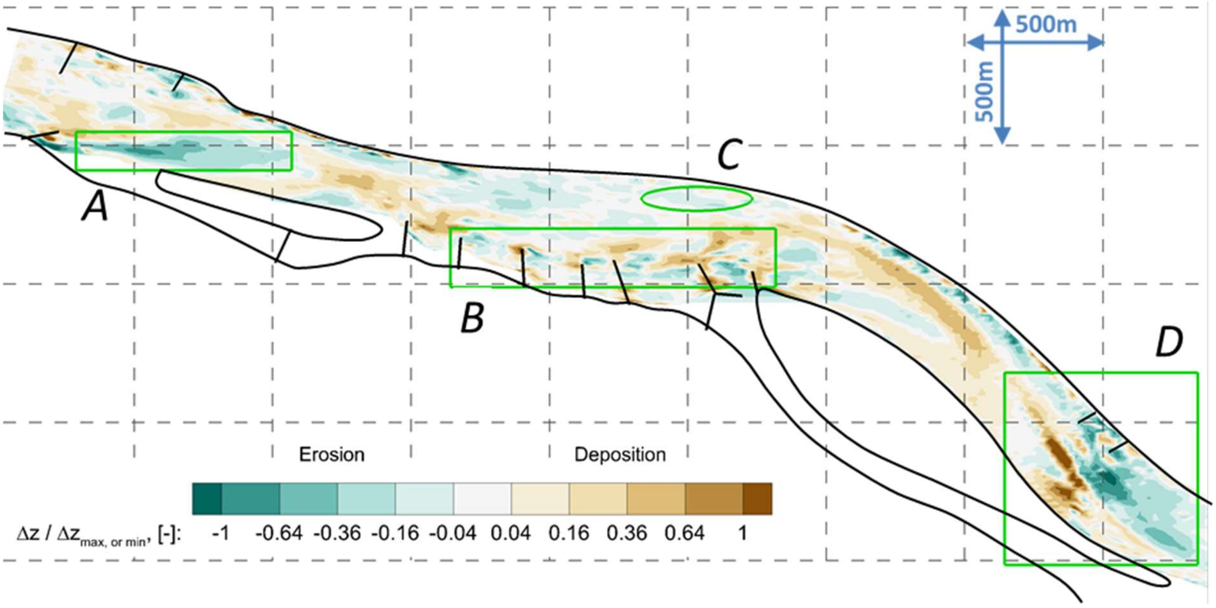

Figure 12. Normalized bed changes of the measured values (0) regarding to the whole period 2012 October – 2014 October.

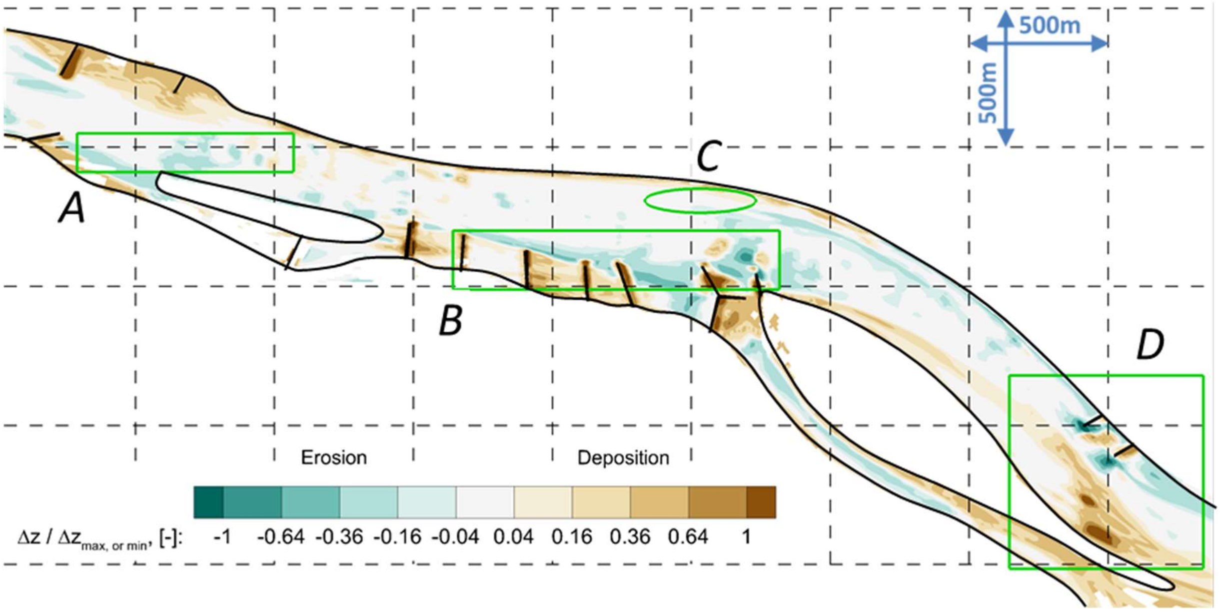

Figure 13. Normalized bed changes of the calculated regarding. The calculation was elaborated for the eight flood waves in the period 2012 October – 2014 October (0).

By the comparison of the measured (0) and calculated normalized bed changes (0) the following remarks can be stated. The modelled bed changes do not represent the remarkable erosion at region *A*. It is noted that this difference also means a sediment supply loss for the downstream in the model calculation. Since the model does not manifest any bed level decreasing, the bed material was probably finer here than it was set in the model. At region *B*, the measured scours appear in the calculated results (blue spots). But not as concentric scours, but rather as lengthwise formations. The numerical model represents depositions closed to the measured magnitude at region B also. However, their location are not accurately; the brown spots occur between the groins, instead of in the front of the groins, like in 0.

Peer-reviewed version available at *Water* **2019**, *11*, 2051; doi:10.3390/w11102051

At the gravel bar in region *C*, negligible bed changes were measured. Likewise, the numerical model predicts stable bed surface. Finally, the combined method points out the growing of the lower part of the Vének lower gravel bar (region *D*, 0). The measured bed changes indicate two, separable depositions. These double depositions are also represented by the model results. Like the measured changes, the model also calculates scouring in the front of the left bank groin pair. However, the extension of it is considerable lower than the scale of the measured deepening. In turn, the lengthwise deposition between the groins (between region *C* and *D*) is also indicated in both measured and calculated maps. However, the calculated deposition occurs in significantly lower range and forms at the right bank side and not in the main stream. Also important match that neither the measured nor the calculated suggests any essential large-scale bed changes in the main channel.

Significant difference between the measured and calculated bed changes happened at region *A*. Here, the effect of the potential error in the initial bed material was further examined. An investigation was performed, which based on the assumption that the initial bed material was set inaccurately around region *A*. The bed material samples around $d_{50} \approx 0.01$m. Considering the grain-size distributions [18], a still realistic, but considerably finer bed material was presupposed. Therefore, the model was set up by 30% lower d_{50}, that is $d_{50} \approx 0.007$m. With this only one difference, the model was run for the historical flood wave. 0 presents the bed changes at region *A*, and at the downstream of it.

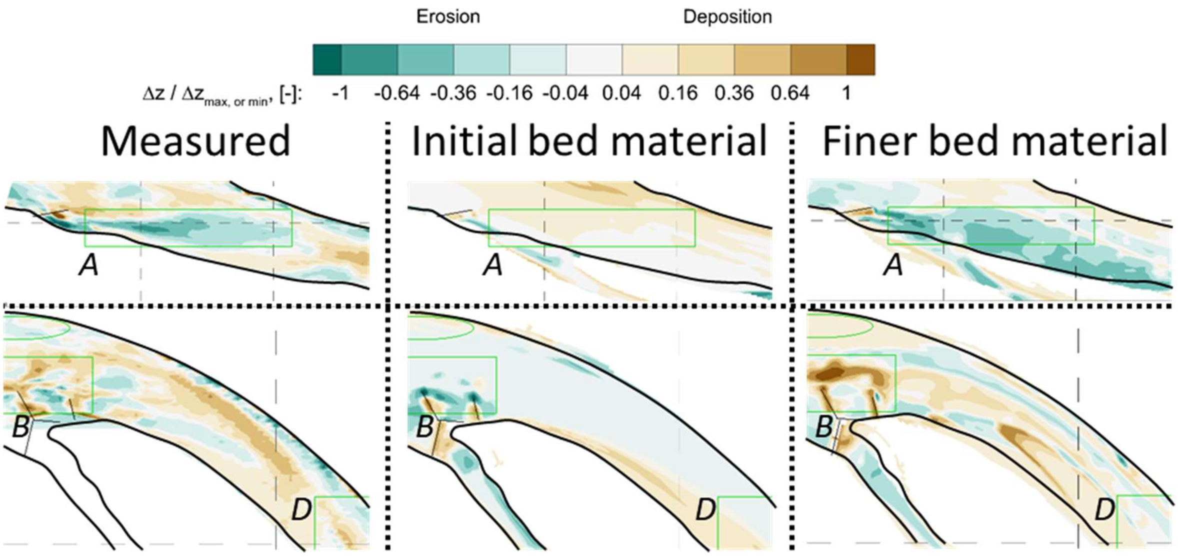

Figure 14. Calculated bed changes by the combining method for the historical flood wave. The model in the middle Figure was set up with the initial, while in the right Figure with finer bed material.

The right side of the Figure shows the bed changes in case of finer bed material. It can be seen that the 30% decrease of the d_{50} resulted in major erosion at region *A*. Considering the measured changes in the left Figure it is obvious that the decreasing of the d_{50} led to a better match to the real bed changes. The lower row of the Figures represents the bed changes at the downstream. Here, important deposition formations could be measured (left Fig.) in front of the right bank groin pair (section *B*) and also in the main stream, between the two gravel bars (between region *B* and *D*). These changes could not be represented by the original model setup (middle Fig.). In turn, in case of finer bed material (right Fig.), the model predicted important depositions at these regions. The extension of the deposition in front of the groin pair (section *B*) is very similar to the measured. And also, the lengthwise extension of the deposition downstream (between region *B* and *D*), in the main stream also reproduced. However, the location of it is not correct. It seems that the model underestimated the crosswise sediment transport, which is a known limitation of the Reynolds averaged description of the flow field [47–50]. Concluding, the herein presented investigation suggests that the bed material at region *A* was finer than the predicted d_{50} allocation for the original model setup. Whit this assumption, the deposition nature at the downstream has become also detectable.

Discussion and conclusion

In this study, the validation of a novel sediment transport approach with field measurements was introduced. The results show that the combined application of the Wilcock and Crowe and the van Rijn models can significantly increase the precision of numerical bed change calculations even by order of magnitude. In addition to the magnitude of local river bed changes, the results also evinced that the location, extension and shape of the bed formations (e.g. scours, deposition, bar evolvement) are much reliably calculated by the novel combined approach than by the previous models. That is, not necessarily the development of completely new models can lead to the evolution of the sediment transport calculation.

There are existing proven models in the literature which works reliably for given morphodynamic cases (e.g. the van Rijn model for hydraulic smooth regimes, which mainly occurs in clear sand bed; or the Wilcock and Crowe model for hydraulic rougher regimes, which develops in coarser bed surfaces). The application of the combined approach really makes sense, within river reaches, where such well-separated morphodynamic situations prevail (e.g. sand aggradation in groin fields; bed armoring in the main stream). In such cases, the local-scale morphodynamic processes are calculated by the proven models, while the interaction between them leads to a more accurate reach-scale calculation. Thus this study highlights that the combined use of sediment transport models is a promising alternative in the sediment transport calculation.

Important to note that the combination of sediment transport models requires an accurate description of the applicability limits of the models. In this study, we used a shear Reynolds number based description. The presented method could be further developed by defining the limits of other models and involving them in combining.

Author Contributions: conceptualization, methodology, software, validation, writing—original draft preparation, visualization, G.T.T., resources, data curation, G.T.T. and S.B.; formal analysis, writing—review and editing, S.B.; supervision, project administration, funding acquisition, S.B. and J.J..

Acknowledgments: This research was supported by MTA TKI of the Hungarian Academy of Sciences. Support of grant BME FIKP-VÍZ by EMMI is also kindly acknowledged. The authors acknowledge the funding of the OTKA FK 128429 grant.

Conflicts of Interest: Declare conflicts of interest or state "The authors declare no conflict of interest." Authors must identify and declare any personal circumstances or interest that may be perceived as inappropriately influencing the representation or interpretation of reported research results. Any role of the funders in the design of the study; in the collection, analyses or interpretation of data; in the writing of the manuscript, or in the decision to publish the results must be declared in this section. If there is no role, please state "The funders had no role in the design of the study; in the collection, analyses, or interpretation of data; in the writing of the manuscript, or in the decision to publish the results".

References

1. Parker, G. Transport of Gravel and Sediment Mixtures. In *Sedimentation Engineering*; Garcia, M., Ed.; American Society of Civil Engineers, 2008; pp. 165–251 ISBN 978-0-7844-0814-8.
2. Meyer-Peter, E.; Müller, R. *Formulas for Bed-Load Transport*; IAHSR 2nd meeting, Stockholm, Sweden, 7-9 June, 1948;
3. Einstein, H.A. *The Bed-Load Function for Sediment Transportation in Open Channel Flows*; Washington, 1950;
4. Ashida, K.; Michiue, M. Study on hydraulic resistance and bedload transport rate in alluvial streams. *Transactions of Japan Society of Civil Engineering* **1972**, *206*, 59–69.
5. Parker, G.; Klingeman, P.; McLean, D. Bedload and size distribution in natural paved gravel bed streams. *Journal of Hydraulic Engineering* **1982**, *108*, 544–571.

Peer-reviewed version available at *Water* **2019**, *11*, 2051; doi:10.3390/w11102051

6. Parker, G. Surface-based bedload transport relation for gravel rivers. *Journal of Hydraulic Research* **1990**, *28*, 417–436.
7. Wilcock, P.R.; Kenworthy, S.T. A two-fraction model for the transport of sand/gravel mixtures. *Water Resources Research* **2002**, *38*, 1–12.
8. Wilcock, P.R.; Crowe, J.C. Surface-based transport model for mixed-size sediment. *Journal of Hydraulic Engineering-Asce* **2003**, *129*, 120–128.
9. Wu, W.; Wang, S.S.Y.; Jia, Y. Nonuniform sediment transport in alluvial rivers. *Journal of Hydraulic Research* **2000**, *38*, 427–434.
10. Powell, D.M.; Reid, I.; Laronne, J.B. Evolution of bed load grain size distribution with increasing flow strength and the effect of flow duration on the caliber of bed load sediment yield in ephemeral gravel bed rivers. *Water Resources Research* **2001**, *37*, 1463–1474.
11. Török, G.T.; Baranya, S.; Rüther, N. 3D CFD Modeling of Local Scouring, Bed Armoring and Sediment Deposition. *Water* **2017**, *9*, 56.
12. Rákóczi, L.; Sass, J. A Felső-Duna és a Szigetközi mellékágak mederalakulása a dunacsúni duzzasztómű üzembe helyezése után (Changes of the channel of the Hungarian Upper Danube and of the side river arms of the Szigetköz upon putting the Dunacsúny I. river barrage into operati. *Vízügyi Közlemények* **1995**, *77*, 46–75.
13. Hankó, Z. Gondolatok a Duna Szap és Szob közötti szakaszának fejlesztéséről (Considerations related to the development of the Danube reach between Szap and Szob). *Vízügyi Közlemények* **2000**, *82*, 285–299.
14. Holubová, K.; Capeková, Z.; Szolgay, J. Impact of hydropower schemes at bedload regime and channel morphology of the Danube River. In Proceedings of the River Flow 2004: Proceedings of the Second International Conference on Fluvial Hydraulics; CRC Press: Napoli, 2004; pp. 135–142.
15. Baranya, S.; Józsa, J.; Török, G.T.; Ficsor, J.; Mohácsiné Simon, G.; Habersack, H.; Haimann, M.; Riegler, A.; Liedermann, M.; Hengl, M. A Duna hordalékvizsgálatai a SEDDON osztrák-magyar együttműködési projekt keretében (Introduction of the joint Austro-Hungarian sediment research under the SEDDON ERFE-project). *Hidrológiai Közlöny* **2015**, *95*, 41–46.
16. Hankó, Z.; Starosolszky, Ö.; Bakonyi, P. Megvalósíthatósági tanulmány a Duna környezetének és hajózhatóságának fejlesztésére (Danube Environmental and navigation Project, Feasibility Study). *Vízügyi Közlemények* **1996**, *78*, 291–315.
17. Goda, L. A Duna gázlói Pozsony-Mohács között (Shallows of the River Danube between Pozsony, Bratislava and Mohács. *Vízügyi Közlemények* **1995**, *77*, 71–102.
18. Török, G.T.; Baranya, S. Morphological Investigation of a Critical Reach of the Upper Hungarian Danube. *Periodica Polytechnica Civil Engineering* **2017**, *61*, 752–761.
19. Holubová, K.; Comaj, M.; Lukac, M.; Mravcová, K.; Capeková, Z.; Antalová, M. *Final report in DuRe Flood*

Peer-reviewed version available at *Water* **2019**, *11*, 2051; doi:10.3390/w11102051

project - 'Danube Floodplain Rehabilitation to Improve Flood Protection and Enhance the Ecological Values of the River in the Stretch between Sap and Szob; Bratislava, 2015;

20. Varga-Lehofer, D.T. A felső-magyarországi Duna morfológiai változásainak elemzése (Investigation of the morphological changes of the Hungarian Upper Danube), BSc Thesis, manuscriprt: Budapest Univerity of Technology and Economics, 2014.
21. Török, G.T.; Józsa, J.; Baranya, S. A Shear Reynolds Number-Based Classification Method of the Nonuniform Bed Load Transport. *Water* **2019**, *11(1)*, 1–16.
22. Liedermann, M.; Gmeiner, P.; Kreisler, A.; Tritthart, M.; Habersack, H. Insights into bedload transport processes of a large regulated gravel-bed river. *Earth Surface Processes and Landforms* **2017**.
23. Baranya, S. Three-dimensional analysis of river hydrodynamics and morphology, PhD Thesis, manuscriprt: Budapest University of Technology and Economics, 2009.
24. Török, G.T.; Baranya, S. A shear Reynolds number based sediment transport classification method for complex river beds. In Proceedings of the 8th International Symphosium on Environmental Hydraulics; 2018.
25. Rákóczi, L. *A Duna Szap-Gönyű közötti szakaszának hajózási viszonyait javító beavatkozások vizsgálata (Investigation of interventions for navigation improvment at the Danube channel between Szap and Szob)*; Technical report, 2004;
26. Baranya, S.; Goda, L.; Józsa, J.; Rákóczi, L. Complex hydro- and sediment dynamics survey of two critical reaches on the Hungarian part of river Danube. *IOP Conference Series: Earth and Environmental Science* **2008**, *4*.
27. Egiazaroff, I. V. Calculation of Nonuniform Sediment Concentrations. *Journal of the Hydraulics Division* **1965**, *91*, 225–247.
28. Bogárdi, J. *A hordalékmozgás elmélete*; Vilmos, I., Ed.; Akadémiai Kiadó: Budapest, Hungary, 1955;
29. van Rijn, L.C. Sediment Transport, Part I: Bed Load Transport. *Journal of Hydraulic Engineering* **1984**, *110*, 1431–1456.
30. van Rijn, L.C. Mathematical modelling of morphological processes in the case of suspended sediment transport. *Delft Hydra. Communication* **1987**.
31. Reidar B. Olsen, N. *A Three-Dimensional Numerical Model for Simulation of Sediment Movements in Water Intakes with Moving Option*; Trondheim, 2002;
32. Olsen, N.R.B. *Numerical Modelling and Hydraulics*; Online manuscript, 2012;
33. Pope, S.B. *Turbulent Flows*; Cambridge University Press, 2000; ISBN 9780521598866.
34. Patankar, S. V. *Numerical Heat Transfer and Fluid Flow*; Minkowycz, M.J., Sparrow, E.M., Eds.; McGraw-

Peer-reviewed version available at *Water* **2019**, *11*, 2051; doi:10.3390/w11102051

Hill Book Company, 1980; ISBN 0-07-048740-5.

35. Schlichting, H. *Boundary-layer theory*; McGraw-Hill: New York, 1979;

36. Zinke, P.; Olsen, N.R.B.; Bogen, J.; Rüther, N. 3D modelling of the flow distribution in the delta of Lake Øyeren, Norway. *Hydrology Research* **2010**, *41*, 92–103.

37. Török, G.T.; Baranya, S.; Rüther, N. Three-dimensional numerical modeling of non-uniform sediment transport and bed armoring process. In Proceedings of the 18th Congress of the Asia & Pacific Division of the International Association for Hydro-Environment Engineering and Research 2012; Jeju, 2012.

38. Fischer-Antze, T.; Reidar B. Olsen, N.; Gutknecht, D. Three-dimensional CFD modeling of morphological bed changes in the Danube River. **2008**, *44*, 1–15.

39. Baranya, S. River Bed Material Mapping to Support Habitat Assesment in Large Rivers. In Proceedings of the 12th International Symposium on Ecohydraulics; Tokyo, Japan, 2018.

40. BME-VVT; OVF; VIZITERV-Environ Kft *A mértékadó árvízszintek országos felülvizsgálata (Reconsideration of the high water levels in Hungary)*; Budapest, Hungary, 2014;

41. Ficsor, J. Lebegtetett hordalék vizsgálata a Felső-magyarországi Duna-szakaszon (Study of suspended sediment transport on the upper Hungarian reach of the Danube River), Thesis, manuscript: Budapest University of Technology and Economics, 2016.

42. Török, G.T. Methodological improvement of morphodynamic investigation tools for rivers with non-uniform bed material by, PhD Thesis, manuscript: Budapest Univerity of Technology and Economics, 2018.

43. Baranya, S.; Józsa, J. Flow analysis in River Danube by field measurement and 3D CFD turbulence modelling. **2006**, *50*, 57–68.

44. Baranya, S.; Józsa, J. Numerical and laboratory investigation of the hydrodynamic complexity of a river confluence. *Periodica Polytechnica Civil Engineering* **2007**, *51*, 3–8.

45. Török, G.T. Vegyes szemcseösszetételű folyómedrek numerikus vizsgálata (Numerical investigation of non-uniform river bed). *Hidrológiai Tájékoztató* **2013**, 22–24.

46. Török, G.T.; Baranya, S.; Rüther, N. Validation of a combined sediment transport modelling approach for the morphodynamic simulation of the upper Hungarian Danube River. In Proceedings of the 19th EGU General Assembly; Vienna, Austria, 2017; Vol. 19:15749.

47. Koken, M.; Constantinescu, G. An investigation of the flow and scour mechanisms around isolated spur dikes in a shallow open channel : 1 . Conditions corresponding to the initiation of the erosion and deposition process. *Water Resources Research* **2008**, *44*, 1–19.

48. Catalano, P.; Wang, M.; Iaccarino, G.; Moin, P. Numerical simulation of the flow around a circular cylinder at high Reynolds numbers. *International Journal of Heat and Fluid Flow* **2003**, *24*, 463–469.

Peer-reviewed version available at *Water* **2019**, *11*, 2051; doi:10.3390/w11102051

49. Roulund, R.; Sumer, B.M.; Fredsøe, J.; Michelsen, J. Numerical and experimental investigation of flow and scour around a circular pile. *Journal of Fluid Mechanics* **2005**, *534*, 351–401.

50. Baranya, S.; Olsen, N.R.B.; Stoesser, T.; Sturm, T. Three-dimensional rans modeling of flow around circular piers using nested grids. *Engineering Applications of Computational Fluid Mechanics* **2012**, *6*, 648–662.